Journal of ELECTRONIC MATERIALS, Vol. 44, No. 6, 2015
DOI: 10.1007/s11664-014-3471-0

Influence of Postdeposition Cooling Atmosphere on Thermoelectric Properties of 2% Al-Doped ZnO Thin Films Grown by Pulsed Laser Deposition

S. SAINI,[1,6] P. MELE,[1,7] H. HONDA,[2] K. MATSUMOTO,[3] K. MIYAZAKI,[3] L. MOLINA LUNA,[4] and P.E. HOPKINS[5]

1.—Institute for Sustainable Sciences and Development, Hiroshima University, Higashi-Hiroshima 739-8530, Japan. 2.—Graduate School for Advanced Sciences of Matter, Hiroshima University, Higashi-Hiroshima 739-8530, Japan. 3.—Kyushu Institute of Technology, Department of Material Science, Kitakyushu 804-8550, Japan. 4.—Department of Materials and Geosciences, Technical University of Darmstadt, Darmstadt, Germany. 5.—Department of Mechanical and Aerospace Engineering, University of Virginia, Charlottesville, USA. 6.—e-mail: ssaini@hiroshima-u.ac.jp. 7.—e-mail: pmele@hiroshima-u.ac.jp

We have investigated the thermoelectric properties of 2% Al-doped ZnO (AZO) thin films depending on the postdeposition cooling atmosphere [in oxygen pressure (AZO-O) or vacuum (AZO-V)]. Thin films were grown by pulsed laser deposition on sapphire (Al_2O_3) substrates at various deposition temperatures (400°C to 600°C). All films were *c*-axis oriented. The electrical conductivity of AZO-V thin films was higher than that of AZO-O thin films across the whole temperature range from 300 K to 600 K, due to the optimal carrier concentration ($10^{20}\,cm^{-3}$) of AZO-V samples. Furthermore, the thermoelectric performance of AZO-V films increased with the deposition temperature; for instance, the highest power factor of $0.87 \times 10^{-3}\,W\,m^{-1}\,K^{-2}$ and dimensionless figure of merit of 0.07 at 600 K were found for AZO-V thin film deposited at 600°C.

Key words: *c*-Axis orientation, Al-doped ZnO thin films , pulsed laser deposition, Seebeck coefficient, power factor, thermoelectric oxides

INTRODUCTION

ZnO is an *n*-type semiconductor with a wide direct bandgap (3.3 eV) which has always attracted much attention because of its versatile applications, e.g., in optical devices for use in the ultraviolet region,[1] piezoelectric transducers,[2] transparent electrodes for solar cells,[3] and gas sensors.[4] Apart from this, ZnO is a good candidate for thermoelectric applications[5–7] since it is low cost, nontoxic, and stable over a wide temperature range (decomposition temperature above 2000°C). Several reports have been published on sintered ZnO with various dopants added to improve its thermoelectric performance. A comprehensive review on bulk ZnO thermoelectric can be found in Ref. 8. In recent years, many research groups have intensively investigated growth of high-quality ZnO thin films for various applications using various oxygen pressures.[9,10] Thin films are advantageous over bulk materials because of their light weight, quick response time, and compact size for use in modules or sensors. Thermoelectric ZnO thin films have not been sufficiently explored, even though they are relatively easy to prepare.[11] The main reason is the practical difficulties in the measurement of thermoelectric properties at high temperature.

Recently, we reported the thermoelectric properties of AZO thin films on different substrates and achieved the highest power factor.[12,13] In this study, we extend our work and discuss the thermoelectric properties of 2% Al-doped ZnO thin films (AZO)

S. Saini and P. Mele contributed equally to this paper.
(Received June 27, 2014; accepted October 11, 2014; published online November 4, 2014)

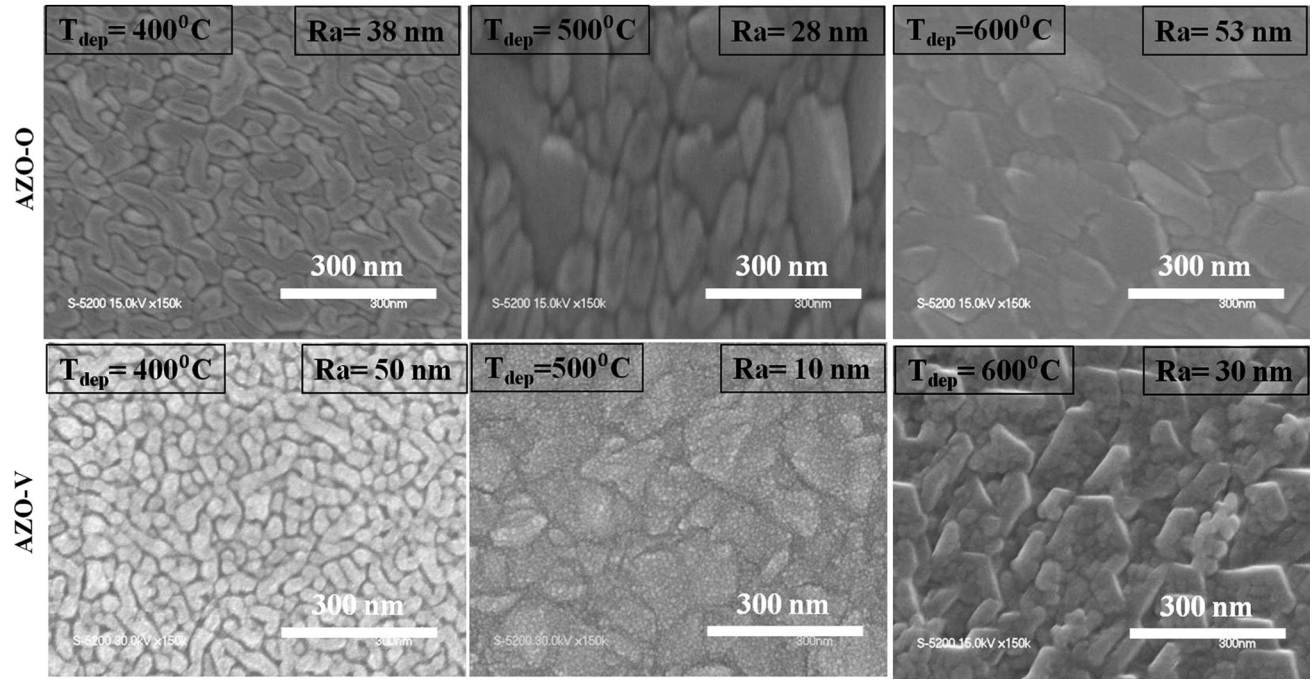

Fig. 1. SEM images of thin films cooled in oxygen atmosphere (AZO-O) or vacuum (AZO-V) after deposition at different temperatures (400°C, 500°C, and 600°C).

deposited by pulsed laser deposition (PLD) on Al_2O_3 single-crystal substrates, with special regard to the effect of the postdeposition cooling atmosphere, which helps to tune the carrier concentration of the thin films.

EXPERIMENTAL PROCEDURES

Al-doped ZnO thin films were deposited by the PLD technique using a Nd:YAG laser (266 nm, 10 Hz) on Al_2O_3 (sapphire, 001) single-crystal substrates at T_{dep} = 400°C, 500°C, and 600°C under oxygen pressure of 200 mTorr. A hard pellet of $Zn_{0.98}Al_{0.02}O$ (20 mm diameter, 3 mm thickness) was prepared by spark plasma sintering and used as a target to grow the thin films by PLD. A detailed description of the sintered target growth is reported elsewhere.[14] The target was rotated during irradiation by the laser beam. The Al_2O_3 substrates were glued with silver paste onto Inconel plate customized for ultrahigh-vacuum applications. The deposition parameters were frequency of 10 Hz, deposition time of 15 min to 30 min, target–substrate distance of 30 mm to 35 mm, and target rotation speed of 30% rpm. The laser was aimed at the dense AZO target with energy density of about 4.2 J/cm^2.

After deposition, we adopted two different cooling patterns to form two series of thin films. However, the cooling rate for both series of thin films was kept the same at 5.5°C/min. The first series comprised AZO films cooled in an oxygen environment ($P_{O_2} \approx$ 300 Torr); these films are named AZO-O hereinafter (thickness ~500 nm). The second series comprised AZO films cooled in vacuum ($P \approx 7.5 \times 10^{-5}$ Torr); these films are named AZO-V hereinafter (thickness ~470 nm).

Structural characterization was performed by x-ray diffraction (XRD) analysis (Bruker D8 Discover), and morphology was checked by scanning electron microscopy (SEM, JEOL, FESEM). The thickness and in-plane roughness were obtained by using a Keyence VK-9700 3D microscope. The electrical conductivity was measured from 300 K to 600 K using a custom-built four-point probe setup based on a current source (ADCMT 6144), a temperature controller (Cryo-con 32), and a nanovoltmeter (Keithley 2182A). The Seebeck coefficient was measured from 300 K to 600 K using a commercially available system (MMR Technologies SB-100). Carrier concentrations at room temperature were evaluated by means of a Quantum Design PPMS. The thermal conductivities of thin films at room temperature were measured by time-domain thermoreflectance (TDTR).[15–17]

RESULTS AND DISCUSSION

The surface morphology of the thin films changed with the deposition temperature. SEM images of various samples are shown in Fig. 1. Independently of the cooling conditions, the grain size increased with the deposition temperature. The morphology evolved from small, elongated grains (length ≈30 nm to 60 nm, at 400°C) to larger grains (length ≈100 nm, at 500°C) and eventually hexagonal grains (side ≈50 nm to 120 nm, at 600°C). Comparing the two series of samples, AZO-O films deposited at 400°C and 500°C showed several pores, while the film deposited at 600°C was well connected. In the case of

AZO-V thin films, pores were always absent and grains were highly connected for all deposition temperatures.

In the θ–2θ scans (not shown here, reported previously[12] for AZO-O thin films), only (002) peaks belonging to hexagonal wurtzite structure were present, so the AZO thin films grew epitaxially with c-axis alignment. The intensity of the (002) peak decreased with increasing deposition temperature for both AZO-O and AZO-V thin films. This indicates that the crystallinity of the films was higher for low deposition temperature and became increasingly poor with increasing deposition temperature. This is confirmed by the increasing value of the full-width at half-maximum (FWHM) of the ω (002) rocking curve with deposition temperature (Table I).

The XRD patterns (ϕ scans) of the thin films are shown in Fig. 2. Independently of the cooling conditions, the films deposited at 400°C showed sixfold symmetry with the six peaks shifted by 30° with respect to the peaks of the Al_2O_3 substrate (not shown here). This rotation enables the minimum epitaxial strain of 19%. With increasing T_{dep}, the alignment of the AZO on the Al_2O_3 became poor, with decreasing peak intensity in 2θ scans. For AZO-O deposited at 500°C, six additional peaks were present, indicating a mixed structure with 30° rotated and unrotated hexagonal unit cells on Al_2O_3.

The transport and thermoelectric properties of the AZO-O and AZO-V thin films are summarized in Table I and plotted in Fig. 3 for the temperature range from 300 K to 600 K. The electrical conductivity of AZO-O thin films (Fig. 3a) increased with temperature, a typical semiconductor behavior. Thin film deposited at 400°C showed the highest electrical conductivity of 415 S/cm at 300 K and 428 S/cm at 600 K. The AZO-V thin films showed metallic behavior, as the electric conductivity decreased with increase in temperature (as shown in Fig. 3c and clear from Table I). AZO-V thin film deposited at 400°C showed the highest electrical conductivity of 742 S/cm at 300 K and 703 S/cm at 600 K. The value of electrical conductivity is higher for AZO-V than AZO-O thin films for given deposition temperature over the whole temperature range from 300 K to 600 K.

Figure 3 also shows a plot of the Seebeck coefficient versus temperature in the range from 300 K to 600 K. All films showed negative Seebeck coefficient, indicating n-type conduction due to oxygen vacancies and Al^{3+} doping. The absolute value of the Seebeck coefficient increased with the deposition temperature for both series of thin films, showing the opposite behavior with respect to the electrical conductivity. The Seebeck coefficient was found to be higher for samples deposited at 600°C. The highest value of the Seebeck coefficient was −92 μV/K at 300 K (and −183 μV/K at 600 K) for AZO-O thin film (Fig. 3b) deposited

Table I. Electrical and thermal parameters at 300 K/600 K for thin films cooled in oxygen atmosphere or vacuum after deposition at different temperatures of 400°C, 500°C, and 600°C

T_{dep}	Cooling Atmosphere	Grain Size (nm)	FWHM (°)	Electrical Conductivity, σ (S/cm)	Carrier Concentration, n (10^{19} cm^{-3})	Seebeck Coefficient, S (μV/K)	Power Factor, PF (10^{-3} W m^{-1} K^{-2})	Thermal Conductivity, κ (W m^{-1} K^{-1})	Figure of Merit, ZT
400°C	Oxygen	60	1.89	299/291	1.1	−58/−126	0.14/0.64	6.9	0.004/0.04
500°C	Oxygen	90	2.01	49/54	0.8	−92/−183	0.04/0.18	6.9	0.002/0.016
600°C	Oxygen	120	2.52	82/96	0.5	−74/−125	0.05/0.15	5.65	0.002/0.016
400°C	Vacuum	30	2.09	742/703	10.0	−36/−78	0.09/0.43	7.17	0.004/0.04
500°C	Vacuum	100	2.17	351/341	7.0	−67/−120	0.16/0.49	6.39	0.007/0.05
600°C	Vacuum	50	4.06	520/485	7.0	−68/−134	0.24/0.87	7.68	0.009/0.07

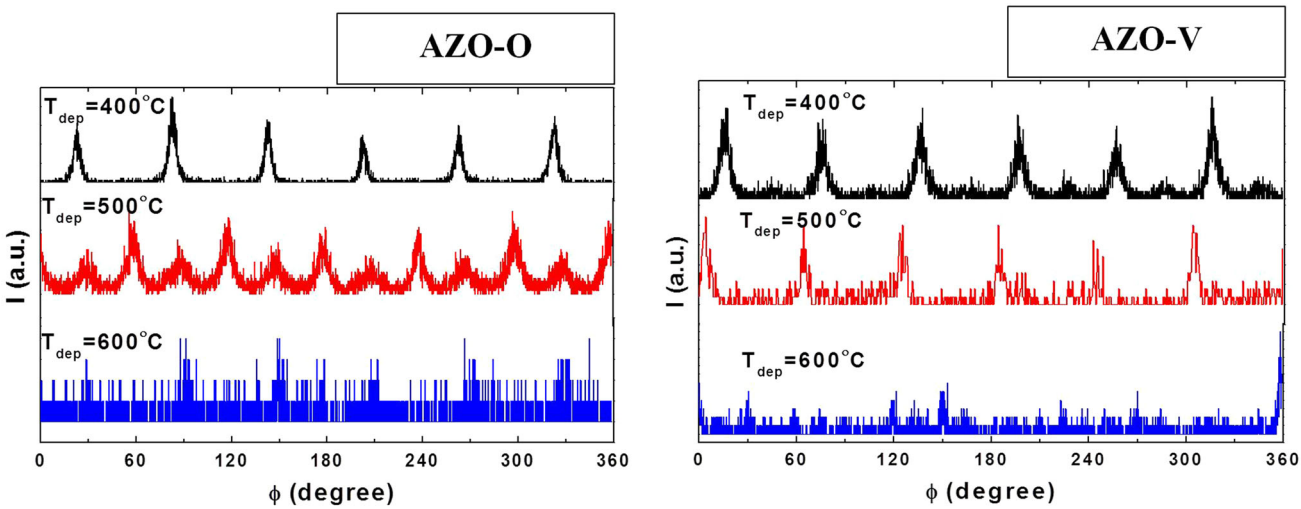

Fig. 2. X-ray diffraction patterns (ϕ scans) of thin films cooled in oxygen atmosphere or vacuum after deposition at different temperatures (400°C, 500°C, and 600°C).

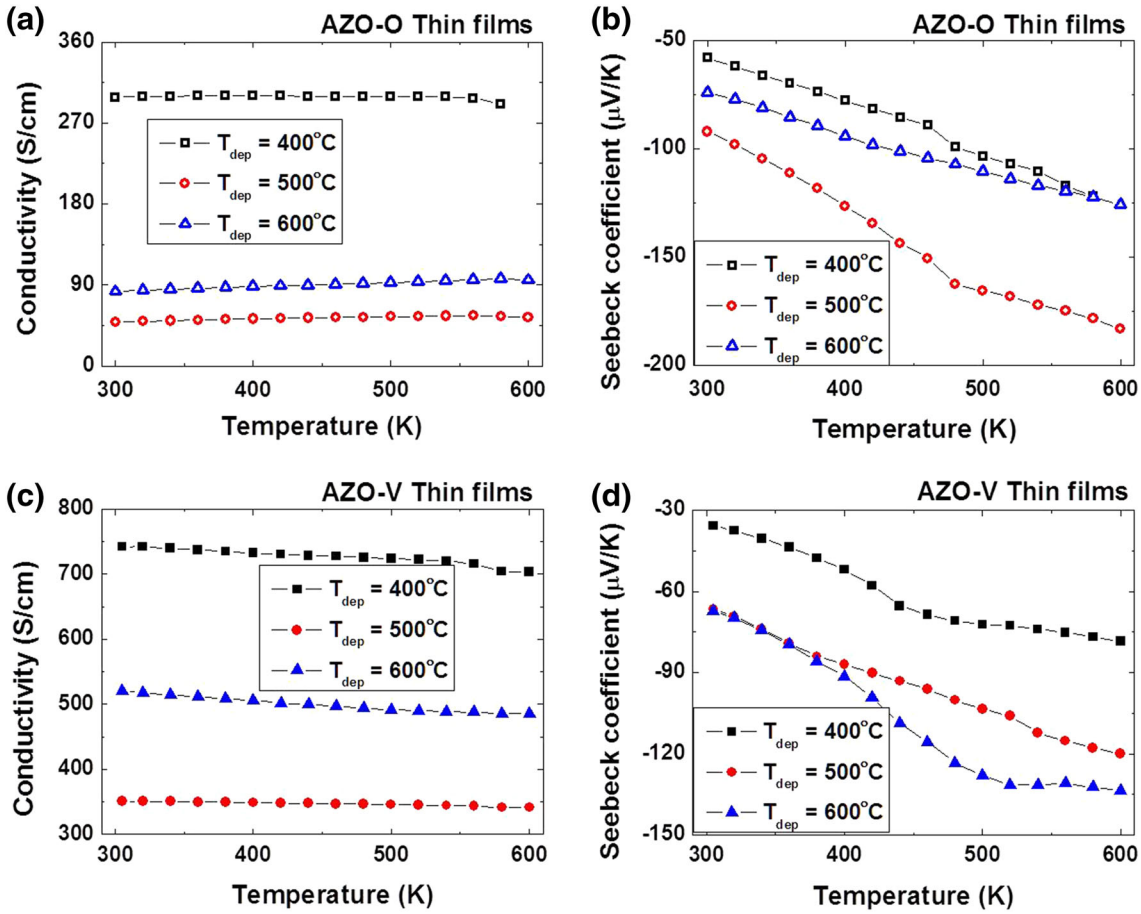

Fig. 3. Electrical conductivity and Seebeck coefficient of thin films cooled in (a, b) oxygen atmosphere or (c, d) vacuum after deposition at different temperatures (400°C, 500°C, and 600°C).

at 500°C and −68 μV/K at 300 K (and −134 μV/K at 600 K) for AZO-V thin film (Fig. 3d) deposited at 600°C.

The efficiency of a thermoelectric material can be determined from the value of the power factor, PF = $\sigma \cdot S^2$, where σ is the electrical conductivity and

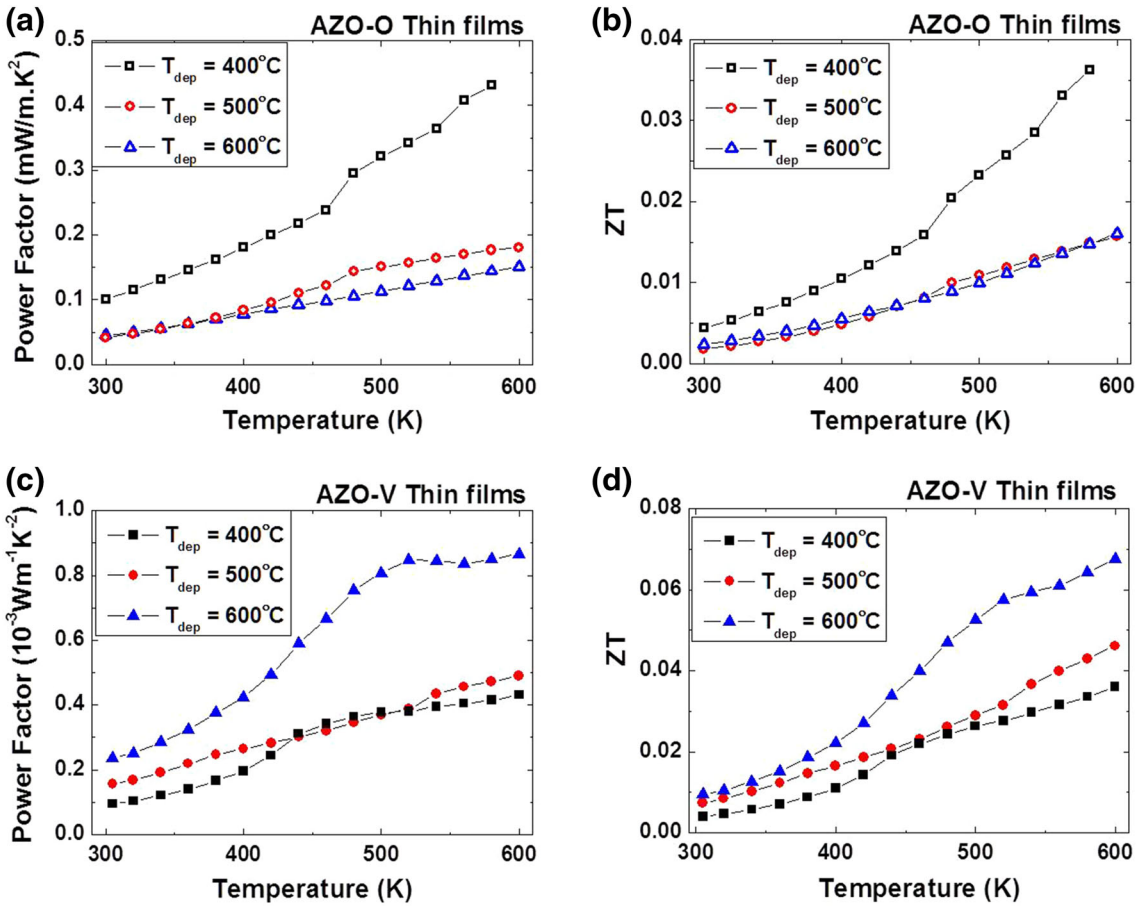

Fig. 4. Power factor and dimensionless figure of merit ZT of thin films cooled in (a, b) oxygen atmosphere or (c, d) vacuum after deposition at different temperatures (400°C, 500°C, and 600°C).

S is the Seebeck coefficient. The power factor values are reported in Table I and shown in Fig. 4 for AZO-O (Fig. 4a) and AZO-V (Fig. 4c) thin films for the temperature range from 300 K to 600 K. The value of the power factor is ruled by the electrical conductivity, decreasing with an increase of deposition temperature for AZO-O thin films but increasing with deposition temperature for AZO-V thin films. AZO-V thin film deposited at 600°C showed the best power factor of $0.24 \times 10^{-3}\,\mathrm{W\,m^{-1}\,K^{-2}}$ at 300 K and $0.87 \times 10^{-3}\,\mathrm{W\,m^{-1}\,K^{-2}}$ at 600 K.

We measured the thermal conductivity (κ) by the TDTR technique at 300 K. The value of the thermal conductivity is reported in Table I. The value of the thermal conductivity was found to be higher for the AZO-V thin films. The value of κ was one order of magnitude lower than for bulk AZO ($34\ \mathrm{W\,m^{-1}\,K^{-2}}$[14]) at room temperature, and is expected to decrease with increase in temperature. The reduction of κ can be attributed to enhanced phonon scattering due to the variety of nanosized grains in the films, as shown in the SEM images (Fig. 1). At this stage, we cannot specify a clear trend for the relation between the thermal conductivity and the different film morphologies.

Furthermore, the dimensionless figure of merit $ZT = (\sigma \cdot S^2) \cdot T/\kappa$ (where S is the Seebeck coefficient, σ is the electrical conductivity, κ is the thermal conductivity, and T is absolute temperature)[18] was calculated and is reported in Table I. The behavior of ZT for the thin films at elevated temperatures was estimated using the κ value at 300 K ($\kappa_{300\mathrm{K}}$) and is shown in Fig. 4b for AZO-O thin films and in Fig. 4d for AZO-V thin films. This approach was used as the thermal conductivity is supposed to decrease with increasing temperature.[19] AZO-V thin film deposited at 600°C showed the best ZT value of 0.009 among all the thin films at 300 K, with a predicted enhancement up to 0.07 at 600 K. This value is still low for practical applications. It could be improved by using a nanoengineering approach, for example, through the introduction of artificial nanodefects to reduce the thermal conductivity.

Figure 5 summarizes the electrical conductivity, carrier concentration, and energy barrier with respect to the FWHM of the ω (002) rocking curve and the lateral grain size of the thin films. The energy barrier of grain boundary against carrier transport can be calculated using Seto's model[20] as $\mu = \frac{eL}{\sqrt{2\pi m^* kT}} \exp\left(\frac{E_b}{kT}\right)$, where μ is the carrier mobility, m^* is the effective mass,

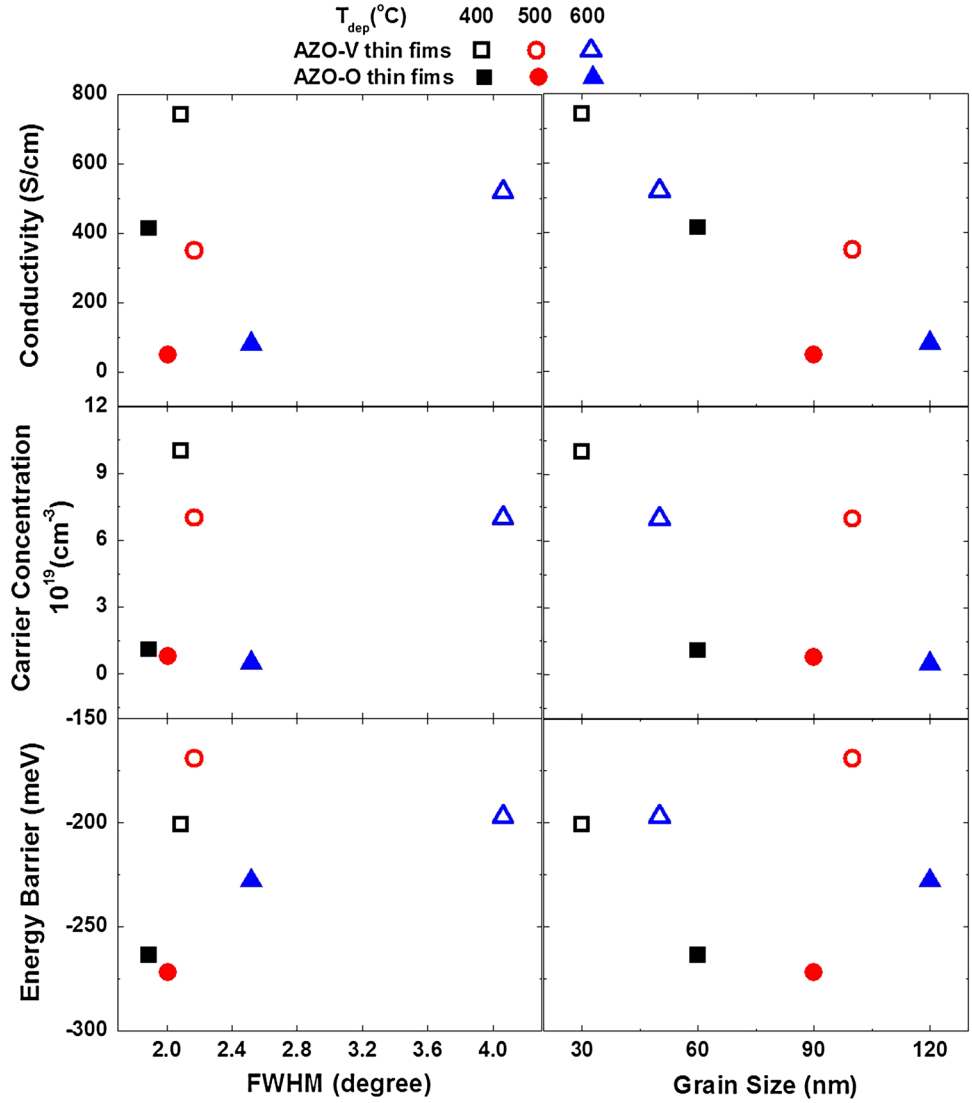

Fig. 5. Electrical conductivity, carrier concentration, and energy barrier of thin films cooled in oxygen atmosphere (filled symbols) or vacuum (empty symbols) after deposition at different temperatures of 400°C (black color), 500°C (red color), and 600°C (blue color), in terms of the FWHM of the ω (002) peak in the x-ray diffraction rocking curve and the lateral grain size (Color figure online).

k is the Boltzmann constant, e is the electron charge, L is the grain size, and E_b is the energy barrier to carrier transport through the grain boundary. The energy barrier defines the collision of electrons with defects along grain boundaries, which leads to the electrical conductivity of the thin films. The conductivity is higher when the absolute value of the energy barrier goes down. Consistently, the AZO-V thin films had lower absolute energy barrier values and higher electrical conductivity.

Further consideration shows that, for both the AZO-O and AZO-V series, the electrical conductivity was larger at lower $T_{dep} = 400°C$, for which the crystallinity was higher as shown in the ϕ scan (Fig. 2). Indeed, over the whole range from 300 K to 600 K, the electrical conductivity of the AZO-V films was superior to that of AZO-O films deposited at the same temperature (Table I). This is due to the effect of the cooling atmosphere. The AZO-V thin films were cooled in vacuum, which led to an increase of the amount of oxygen vacancies.[9,21] Consistently, the carrier concentration of the AZO-V thin films was large, being about 10^{20} cm^{-3}, which is considered ideal for thermoelectric materials.[22] In comparison, the carrier concentration of the AZO-O films was one or two orders of magnitude lower, so the electrical conductivity was lower, especially for $T_{dep} > 400°C$.

CONCLUSIONS

We successfully grew c-axis-oriented 2% Al-doped ZnO (AZO) thin films by the PLD technique at various deposition temperatures on sapphire substrate. Their structure, morphology, and thermoelectrical properties were studied depending on the cooling atmo-

sphere used. Compared with films cooled in oxygen atmosphere (AZO-O), thin films cooled in vacuum (AZO-V) showed metallic behavior with high electrical conductivity in the range from 300 K to 600 K. This behavior is related to the enhanced carrier concentration (on the order of 10^{20} cm^{-3}). The value of κ was one order of magnitude lower than for bulk AZO ($34\ W\,m^{-1}\,K^{-2}$) at room temperature. The thermoelectric performance was also greatly improved by vacuum postdeposition cooling; the power factor of the best AZO-V film was $0.87 \times 10^{-3}\ W\,m^{-1}\,K^{-2}$ at 600 K. The best figure of merit ZT values for thin films at elevated temperatures across the whole temperature range was shown by the AZO-V thin film deposited at 600°C (ZT = 0.07 at 600 K).

ACKNOWLEDGEMENTS

We thank Prof. T. Suzuki, Prof. T. Takabatake and Prof. T. Suekuni, AdSM, Hiroshima University, for their kind support on experimental techniques and measurements.

REFERENCES

1. G.M. Ali and P. Chakrabarti, *J. Phys. D: Appl. Phys*. 43, 415103 (2010).
2. P.X. Gao and Z.L. Wang, *J. Appl. Phys*. 97, 044304 (2005).
3. M. Law, L.E. Greene, J.C. Johnson, and R. Saykally, P. Yang, *Nat. Mater*. 4, 455 (2005).
4. M. Kaur, S.V.S. Chauhan, S. Sinha, M. Bharti, R. Mohan, S.K. Gupta, and J.V. Yakhmi, *J. Nanosci. Nanotechnol*. 9, 5293 (2009).
5. M. Ohtaki, T. Tsubota, K. Eguchi, and H. Arai, *J. Appl. Phys*. 79, 1816 (1996).
6. J.P. Wiff, Y. Kinemuchi, and K. Watari, *Mater. Lett*. 63, 2470 (2009).
7. A.I. Abutaha, S.R. Sarath Kumar, and H.N. Alshareef, *Appl. Phys. Lett*. 102, 053507 (2013).
8. J.W. Fergus, *J. Eur. Ceram. Soc*. 32, 525 (2012).
9. R. Honga, H. Qia, J. Huanga, H. Hea, Z. Fana, and J. Shaoa, *Thin Solid Films* 473, 58 (2005).
10. F.K. Shan, G.X. Liu, W.J. Lee, and B.C. Shin, *J. Appl. Phys*. 101, 053106 (2007).
11. B. Singh, Z.A. Khan, I. Khan, and S. Ghosh, *Appl. Phys. Lett*. 97, 241903 (2010).
12. P. Mele, S. Saini, H. Honda, K. Matsumoto, K. Miyazaki, H. Hagino, and A. Ichinose, *Appl. Phys. Lett*. 102, 253903 (2013).
13. S. Saini, P. Mele, H. Honda, D.J. Henry, P.E. Hopkins, L.M. Luna, K. Matsumoto, K. Miyazaki, and A. Ichinose, *Jpn. J. Appl. Phys*. 53, 060306 (2014).
14. P. Mele, K. Matsumoto, T. Azuma, K. Kamesawa, S. Tanaka, J. Kurosaki, and K. Miyazaki, *Mater. Res. Soc. Symp. Proc*. 1166, 3 (2009).
15. D.G. Cahill, K.E. Goodson, and A. Majumdar, *J. Heat Transf*. 124, 223241 (2002).
16. A.J. Schmidt, X. Chen, and G. Chen, *Rev. Sci. Instrum*. 79, 114902 (2008).
17. P.E. Hopkins, J.R. Serrano, L.M. Phinney, S.P. Kearney, T.W. Grasser, and C.T. Harris, *J. Heat Transf*. 132, 081302 (2010).
18. H. Böttner, *Mater. Res. Soc. Symp. Proc*. 1166, N01–01 (2009).
19. G.S. Nolas and H.J. Goldsmid, *Thermal Conductivity: Theory, Properties and Applications* (Kluwer Academic/Plenum, New York, 2004), p. 114.
20. J.Y. Seto, *J. Appl. Phys*. 46, 5247 (1975).
21. K.-K. Kim, S. Niki, J.Y. Oh, J.O. Song, T.Y. Seong, S.J. Park, S. Fujita, and S.W. Kim, *J. Appl. Phys*. 97, 066103 (2005).
22. G.J. Snyder and E.S. Toberer, *Nat. Mater*. 7, 105 (2008).